



Prepared for:

Rijkswaterstaat, Dienst Getijdewateren

The large oscillating water tunnel

Technical specifications and performances

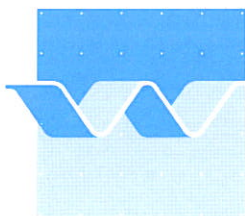
March 1989

	bibliotheek postbus 177 - 2600 MH Delft waterloopkundig laboratorium/WL
BB	0001477
WL	H10480
EXPL	 R0001581

The large oscillating water tunnel

Technical specifications and performances

J.S. Ribberink



delft hydraulics

CONTENTS

	page
1. <u>Introduction</u>	1
2. <u>Technical specifications of the tunnel</u>	3
2.1 General.....	3
2.2 Driving system of the piston.....	3
2.3 Test section.....	4
2.4 Remaining features.....	5
2.5 Measuring possibilities.....	6
3. <u>Performance tests of the tunnel</u>	8
3.1 General.....	8
3.2 Tunnel performance.....	9
3.2.1 Working range.....	9
3.2.2 Signal transfer characteristics.....	10
3.2.3 Oscillatory flow conditions in the test section.....	13
4. <u>Summary and conclusions</u>	15

REFERENCES

FIGURES

1. Introduction

After several years of research experience in the small DELFT HYDRAULICS oscillating water tunnel (1977-1985) in the framework of the Applied Research Program (TOW) of the Dutch Ministry of Transport and Public Works (Rijkswaterstaat), it was decided in 1985 to extend the research of wave induced sea-bed mechanics to controlled simulated field conditions and to build a large oscillating water tunnel.

More background information about the research program as carried out in the small tunnel, research possibilities in the large tunnel and the design characteristics of the new tunnel can be found in Bosman (1985).

Figure 1 (from Bosman, 1985) shows the requirements of the new tunnel, expressed in maximum velocity amplitudes as a function of the oscillation period. In a later stage the primary requirement was chosen for the design, i.e.:

- (wave) periods : $5 < T < 10$ s
- (near-bed orbital) velocity amplitudes : $0 < U < 1.5$ m/s
- basic constructional possibility for bed slopes until 1:20

Figure 1 also shows the working regimes of three other existing tunnels:

- the small tunnel of Delft Hydraulics (see Hulsbergen en Bosman, 1981),
- the large tunnel of the Technical University of Denmark (ISVA, see e.g. Jonsson and Carlsen, 1975), and
- the tunnel of Scripps Institution of Oceanography (see King, Powell and Seymour, 1984).

Moreover, Fig. 1 shows bed (form) regimes (for $D_{50} = .21$ mm), the wave breaking criterion of Miche, regimes of small and large wave flumes and regimes of non-extreme and extreme (Dutch) coastal zone conditions.

It is shown that, contrary to the small tunnel and the Scripps tunnel, the new tunnel should be able to simulate extreme coastal zone conditions.

The ISVA tunnel reaches even more extreme conditions, however, because of an applied soft pneumatic driving system, this tunnel can only produce controlled sinusoidal oscillations near the resonance period of 9.7 s. The new DHL tunnel is provided with a hard hydraulic system and should therefore be able to produce controlled sinusoidal oscillations within the complete working regime. Additionally, the new tunnel should have the possibilities to produce controlled random oscillations (irregularity of waves!).

Figure 1 also shows that the new tunnel should be able to simulate sheet flow conditions, which is considered to be of importance in the light of research of cross-shore sediment transport.

The construction of the new tunnel took place in 1986. A number of performance tests of the tunnel were carried out in 1987 and led to some modifications of the hydraulic driving system and the tunnel geometry.

See Chapter 2 for the technical specifications of the new tunnel and its standard available measuring equipment.

The performance tests (without sand !) were finished in 1988 and are reported in Chapter 3.

A number of conclusions and a summary are given in Chapter 4.

2. Technical specifications of the tunnel

2.1 General

A general outline of the new tunnel and a photographic impression is given in Fig. 2. The tunnel is built in the shape of a flat U-tube with a long rectangular horizontal section (test section) and cylindrical risers on either end. A piston in the closed cylinder is driven by an hydraulic servo-cylinder and generates the oscillating water motion. The piston is in direct contact with the water; O-ring seals prevent the water to enter the space above the piston, which is open to the atmosphere.

Flow straighteners at both ends of the test section are applied for the transition from vertical to horizontal oscillation. The other cylindrical riser is open to the atmosphere.

The tunnel is constructed on a I-beam steel frame which is supported at one side by a pivot for tilting provisions in the future.

The steel vertical cylindrical risers have an inner diameter of 1.0 meter.

The total height of the tunnel is approximately 9.0 meter.

The test section has an approximate length of 15 m, an inner width of 0.3 m and an inner height of 1.1 meter. The lower 0.3 m is available for a sand bed, the upper 0.8 m for the oscillatory flow.

In Section 2.2 the driving system of the piston will be described. In Section 2.3 more details will be given of the test section, while in Section 2.4 some remaining features of the tunnel will be described. In Section 2.5 the presently available measuring possibilities will be given.

This report does not give detailed constructional and operational information but is focussed on those items which are relevant for research workers which plan to use the tunnel. All information concerning tunnel construction, applied mechanical, electrical and electronical devices/instruments is available at the Building and Instrumentation Sections of DELFT HYDRAULICS, de Voorst.

2.2 Driving system of the piston

The main part of the driving system of the tunnel is identical to the driving system of the DELFT HYDRAULICS small water tunnel, which is extensively described by Hulsbergen et al (1981). An outline of the driving system as applied for the large tunnel is given in Fig. 3.

Two main components of the driving system can be distinguished:

- a high pressure hydraulic part, and
- an electric part

The tunnel piston is driven by a hydraulic servo-cylinder mounted on top of the cylindrical riser. The servo-cylinder moves the tunnel piston in response to hydraulic pressure differences which are induced on both sides of the servo-cylinder piston and are controlled by an electric/hydraulic control valve. A hydraulic pump supplies oil to the valve (maximum 57 dm³/min, 170 bar) which allows a maximum piston velocity of 0.53 m/s and a maximum driving force of 30.6 kN (area of servo-cylinder piston $18.01 * 10^{-4}$ m²).

This maximum driving force is available in case of no piston motion; at maximum piston velocity a reduced maximum driving force of 27 kN is still available (caused by friction losses in the hydraulic power system).

The electric hydraulic control valve (see Hulsbergen et al, 1981 for more details) is controlled by an electric signal produced by a servo amplifier. The amplifier subtracts the piston position signal as measured by a potentiometer and the desired piston position signal (from input signal generator); the resulting signal opens en closes high pressure hydraulic ports in the control valve.

The input signal generation (piston position) takes place by an electronic harmonic oscillator (for sinusoidal piston motion with prescribed frequency and amplitude) or with a punch paper tape unit (for prepared time series with for example random oscillations with prescribed peak frequency and energy level).

The piston of the cylindrical riser has a maximum stroke of 1.5 m (i.e. maximum piston amplitude $x_{p_{max}} = 0.75$ m) and a diameter of 1.0 m (area of the piston face = 0.785 m²).

2.3 Test section

The test section is 15.0 m long (including flow straighteners), 1.1 m high and 0.3 m wide. A sand bed with a length of 12.6 m can be made in the test section. The working cross-section is 0.8 m high and 0.3 m wide (0.3 m deep sand bed). This cross-sectional area (= 0.24 m²) is 3.27 times smaller than the cross-sectional area of the driving piston. Consequently the maximum water particle

displacement is 3.27 times greater than the maximum stroke length of the piston and reaches 4.9 meter (app. 1/3 of the test section length). The maximum particle velocity in the test section is 3.27 times the maximum piston velocity and reaches approx. 1.8 m/s.

The side walls of the test section consist of 1.9 cm thick glass windows, supported every 34 cm by steel I-beams. In the central part of the test section a central measuring section is present with 1.0 m long windows supported by horizontal steel I-beams.

The roof of the test section consists of 13 steel sections with a length of 1.0 m which are attached to the test section with steel bolts and can be separately removed (e.g. for sand supply). In the roof sections provisions are taken for the installation of measuring instruments which should operate in the test section. The top of the test section is provided with rails which allows a measuring car (laser-doppler system) to be moved along the complete test section.

During the performance tests a steel dummy bottom (height 0.3 m) was used as replacement of the sand bed.

2.4 Remaining features

The cylindrical risers have the possibility to connect a (recirculating) flow system for the realization of a net current (superimposed upon the oscillatory flow) in the test section.

The tunnel is provided with the following safety arrangements:

- the stroke of the tunnel piston is limited by an electronic limitation of the voltage of generated input signal (± 10 V),
- the piston velocity is limited by the hydraulic power supply, through limitation of the hydraulic fluid discharge into the servo-cylinder (max. piston velocity 0.53 m/s),
- the driving force of the piston is limited by the hydraulic power supply, through limitation of the maximum hydraulic pressure in this system (170 bar),
- an air-intrusion valve, installed in the closed cylindrical riser, allows air to enter the water column below the driving piston when the water pressure reaches a too low value (-0.026 bar),

- a blow-out plug, installed in the closed cylindrical riser, allows the water to leave the tunnel when the pressure inside the tunnel reaches a too high value (2.5 bar), hereby avoiding the over pressure of a water hammer.

Trapped air below the driving piston can be removed with a valve in the piston face. The driving piston is provided with teflon and rubber O-ring seals. Lubrication of the piston/cylinder interface takes place from above with a water sprinkler system. The water above the piston is removed from time to time by an automatic air-driven pump.

A flight of steps around the closed cylinder and along the test section enables an easy access to the main components of the driving system and the measuring instruments in the test section.

Operation of the hydraulic power supply and the water supply to the tunnel takes place near the tunnel. After the tunnel is filled with water and the hydraulic power system is pressurized, the tunnel operation takes place from a measuring office next to the tunnel. Here the desired input signal is generated and moreover measured data can be collected and visualized.

2.5 Measuring possibilities

The tunnel is equipped with a forward-scatter laser-doppler system for the measurement of the horizontal and vertical water velocity components in a desired vertical plane in longitudinal direction of the test section (see Godefroy, 1981 for a detailed description of the basic lda system).

The present system is mounted on the movable measuring car as described above; a positioning system enables velocity measurements in each position in the lower 40 cm of the working cross section along the complete test section.

A movable sand suction system is present inside the test section, which enables the measurement of time (wave) averaged sediment concentration profiles in the central 3.0 m of the test section along the tunnel axis.

For a more detailed description of the transverse suction method of sand see Bosman et al (1987). Figure 4 shows the intake nozzle system with 10 nozzles (inner diameter of the nozzles 3 mm) and an outline of the complete suction system. The nozzle system can be moved along a rail (length 3.0 m), mounted at the ceiling in the central part of the test section, and positioned at a desired fixed position.

For vertical positioning of the suction system the rail can be moved in vertical sense over a distance of 30 centimeter. The mechanical (vertical and horizontal) positioning device is mounted on top of the test section and allows re-positioning of the suction system during tunnel operation. The suction is driven by 10 peristaltic pumps achieving a desired intake velocity. The sand samples are collected in buckets. The sediment concentration can be determined with a calibrated wet-volume measurement technique.

The following electric signals are measured and available in the measuring office:

- the desired input signal for the piston motion,
- the measured piston position,
- the measured piston velocity (time derivative of the piston position),
- the pressure difference in the servo-cylinder (driving pressure),
- the horizontal water velocity component, and
- the vertical water velocity component.

The bottom of the cylindrical risers are provided with valves which enable the removal of trapped sand from the test section and can therefore be applied for the measurement of the sand transport at both ends of the test section.

3. Performance tests of the tunnel

3.1 General

A number of performance tests were carried out with the new tunnel with the aim to gather information on:

- the working range, i.e. is it possible to satisfy the design characteristics (velocity and period range, see Fig. 1)?,
- the signal transfer characteristics, i.e. is the piston motion and the water velocity in the tunnel in accordance with the desired input signal (amplitude, phase transfer and deformation)?,
- the oscillatory flow conditions in the test section.

During these tests the test section of the tunnel was provided with a dummy steel bottom with a height of 0.3 m, leaving a working height of 0.8 m in the tunnel.

The tests were carried out with sinusoidal input signals for the piston motion with:

oscillation periods T in the range 2 - 14 s

piston amplitudes in the range 5 - 100%, i.e. 3.75 - 75 cm (= maximum)

Measurements were carried out of the input signal, the piston displacement and piston velocity, the pressure difference in the servo-cylinder (driving force) and the water velocity in the tunnel using measurement techniques as described in the preceding Chapter.

The tests were repeated several times after the realization of a number of tunnel modifications. The following modifications were carried out:

- the open cylinder was made 1.9 m longer in order to create an extra water column in this cylinder for the compensation of pressure forces in the closed cylinder (piston weight),
- the servo-cylinder was revised for the minimization of oil leakage,
- the suspension of the servo-cylinder was improved after the observation of damage of the connecting rod,
- corrections were made of the hydraulic power unit, i.e. adjustment of the oil discharge limitation (increase of maximum possible piston velocity from 0.48 to 0.53 m/s) and the creation of extra oil pressure expansion buffers,
- an additional O-ring seal was made around the tunnel piston (preventing sand grains access to the piston-cylinder interface) and two existing O-ring seals were renewed,

- a water sprinkler system (for lubrication of the piston-cylinder interface) was installed,
- the frame of the laser-doppler system was strengthened.

Only the latest test results, which show the present tunnel characteristics, are presented in the following section.

3.2 Tunnel performance

3.2.1 Working range

The test experiments indicated that the maximum velocity amplitude which can be realized in the tunnel is determined by (see Fig. 5):

- an acceleration limitation which appears as a coming into operation of the air-intrusion valve (exceedance of under-pressure limit) for oscillation periods $T < 5$ s; this constraint can theoretically be expressed as a linear relation between the maximum velocity amplitude U_{\max} in the test section and the period:

$$U_{\max} = a_{\max} \cdot T/2\pi$$

with:

$$a_{\max} = \text{maximum acceleration} \approx 2 \text{ m/s}^2$$

- the piston displacement limitation for oscillation periods $T > 8$ s, which can be translated to the following constraint for the maximum velocity amplitude:

$$U_{\max} = x_{\max} \cdot 2\pi/T$$

with:

$$\begin{aligned} x_{\max} &= \text{maximum water particle amplitude in the test section} \\ &= x_{p\max} \cdot R \end{aligned}$$

$$x_{p\max} = \text{maximum piston amplitude} (= 75 \text{ cm})$$

$$R = \text{ratio of cross-sectional areas of cylindrical riser and test section} \approx 3.27$$

- the piston velocity limitation as caused by the oil discharge limitation in the hydraulic power system for oscillation periods $5 < T < 8$ s and which can be expressed as:

$$U_{\max} = R \cdot q_{\max} / A_{sc}$$

with:

q_{\max} = maximum oil discharge in the hydraulic power unit $\approx 57 \text{ dm}^3/\text{min}$

A_{sc} = cross-sectional area of the servo-cylinder piston

The maximum water velocity amplitude which can be realized in the test section as a result of these constraints is shown in Fig. 5 as a function of the oscillation period. Comparison with the design graph of Fig. 1 shows that the maximum possible velocity equals or even exceeds the primary requirement.

3.2.2 Signal transfer characteristics

In Fig. 6 two characteristic sets of tunnel signals are shown for the case of sinusoidal input signals with two different oscillation periods ($T = 4$ and 10 s) and almost the same velocity amplitude ($U \approx 1.2 \text{ m/s}$).

Both paper recordings show the piston motion, the piston velocity (phase shift 90°), the driving pressure difference in the servo-cylinder and the horizontal water velocity in the test section (middle of the test section, 40 cm from the bottom).

The case $T = 4 \text{ s}$ is dominated by the inertial forces (acceleration/deceleration of the water mass), which is shown by the 90° phase shift between the piston velocity and the (relatively large) driving force.

The case $T = 10 \text{ s}$ is dominated by frictional forces (e.g. in the flow straighteners) which is shown by the piston velocity being in phase with the (relatively low) driving force.

During inertial force dominance a difference appears in the piston upward and downward motion which is most probably caused by the asymmetry of the tunnel, i.e. the difference between the closed cylindrical riser (driving cylinder) and the open cylinder. As a consequence an asymmetry appears in the driving force which is directly translated into a small deformation of the velocity signal during flow reversal ($U = 0$).

During frictional force dominance a small deformation of the sinusoidal shape of the velocity signal occurs near the crests; this is caused by the fact that the maximum frictional forces occur simultaneously with the maximum velocities.

AMPLITUDE/PHASE TRANSFER

The measured amplitude and phase transfer between input signal and piston displacement is shown in Fig. 7. The upper graph shows the behaviour of amplitude ratio of the piston displacement and the input signal (in Volts/ Volts), the lower graph shows phase-shift between both signals (in seconds). Both parameters are shown as a function of the oscillation period with the relative piston amplitude ($\hat{x}_p/\hat{x}_{p_{\max}}$) as a parameter.

The amplitude ratio varies around a value of 0.9. Although a random measuring error of 2 - 3% is present in the calculated values, a systematic deviation from an ideal linear transfer relation (i.e. a constant amplitude ratio for all periods and amplitudes) can be observed.

This deviation (0 - 5%) especially occurs for:

- small oscillation periods ($T = 4 - 6$ s), which could be caused by the inertial force dominance in this range, and
- small relative piston amplitudes ($\hat{x}_p = 0 - 18$ cm), which is probably caused by frictional forces at the piston-cylinder interface.

The latter deviations are of relatively low importance because of the relatively low water velocities ($U < 0.25$ m/s) in these small amplitude conditions. The deviations in the small period range are considered to be more serious especially in case of controlled random wave simulation in the tunnel.

The piston motion follows the input signal with a relatively small phase lag of 0.2 - 0.3 s (measuring error appr. 10%) in the relevant piston amplitude range (25 - 100%) and with no systematic period influence in the period range 3 - 12 seconds. For smaller piston amplitudes combined with relatively large oscillation periods (> 10 s) a deviation occurs from the ideal phase relation (increased phase lag caused by frictional forces). Nevertheless, in the range of relevant tunnel conditions the deviation of the observed phase transfer from the ideal phase transfer (constant phase shift for all periods and piston amplitudes) is considered to be small.

The signal transfer from piston motion to water motion in the test section of the tunnel can be considered as direct (see also Fig. 6), i.e.:

- a fixed amplitude ratio exists between the piston velocity and the (cross-sectional) averaged water velocity in the test section, which is independent of the oscillation period and the piston amplitude but only depends of the sand bed level in the test section (area of working cross section),
- a negligible phase lag exists between the piston motion and the water motion in the test section.

DEFORMATION

For a selected number of tests energy spectral density functions were determined of the piston velocity signal using a digital signal analyzer. Sinusoidal input signals were used with periods 5, 8, 10 and 14 seconds; the water velocity was varied in the working range (0 - 1.8 m/s). For each spectrum a measured time series of the piston velocity was used with a duration of 250 s which was sampled with a sampling frequency of 4 Hz. Figure 8 shows an example of a measured spectral density function for the case of $T = 8$ s and water velocity amplitude $U = 0.9$ m/s. The horizontal axis shows the frequency between 0 and 1.0 Hz, the vertical axis shows the $10 * 10\log$ of the energy density (in dB). It is shown in Fig. 8 that, although the input signal is almost ideally sinusoidal (higher harmonics $< 0.03\%$), the piston velocity signal contains higher harmonics with frequencies $2f_0, 3f_0, 4f_0$, etc. (with $f_0 =$ frequency of the imposed oscillation $= 1/T = 0.125$ Hz). The importance of the higher harmonics can be estimated by comparing the peak heights in the spectrum with the peak height of the basic oscillation, using the following relation:

$$U_i/U_0 = 10^{\alpha/20}$$

in which:

U_i/U_0 = velocity amplitude ratio of the i -th harmonic and the basic oscillation
 $\alpha = G_i - G_0$ = difference in peak energy density of the i -th harmonic and the basic oscillation (in dB)

In the example of Fig. 8 this leads to a velocity amplitude ratio of 0.32% for the first harmonic ($f_1 = 2 f_0 = 0.25$ Hz) and for the second harmonic ($f_2 = 3 f_0 = 0.375$ Hz). This can be considered as a minor deformation of the basic imposed sinusoidal oscillation.

Figure 9 shows the result of this analysis for the complete set of measurements. The velocity amplitude ratio of the first harmonic (upper graph) and the second harmonic (lower graph) are shown as a function of the water velocity amplitude in the test section for different oscillation periods. It can be observed that:

- the contribution of higher harmonics is always $< 10\%$ and increases for decreasing periods; especially for $T = 5$ s the deformation is considerably higher than for 8, 10 and 14 seconds,

- roughly three velocity ranges can be distinguished:
 - i. a low velocity range ($0 < U < 0.35$ m/s) with a considerable deformation in which the contribution of the first harmonic is $< 1.5\%$ for all periods and the contribution of the second harmonic is $< 6 - 10\%$,
 - ii. a middle velocity range ($0.35 < U < 1.5$ m/s) with a relatively low deformation; the contribution of the first harmonic is $< 1\%$ (for all periods); the contribution of the second harmonic is also $< 1\%$ for the periods 8, 10 and 14 s but $< 6\%$ for $T = 5$ s,
 - iii. a high velocity range ($1.5 < U < 1.9$ m/s) in which the deformation increases again for the periods 6 and 8 seconds (2-8%).

The deformation in the low velocity range is probably caused by the relatively large friction at the piston-cylinder interface. The deformation in the high velocity range and the low period range is probably caused by the increased importance of the inertial forces.

Visual inspection of the time series of the velocity signal learns (see Fig. 6) that the presence of higher harmonics does not lead to the type of asymmetry which can be expected in field conditions, i.e. high (onshore) crest velocities and relatively low (offshore) trough velocities. In stead the 'onshore' and 'offshore' water particle excursions are rather symmetrical with similar velocity amplitudes. This difference in asymmetry type is caused by a difference in phase shift between the basic oscillation and the generated higher harmonics (see also Ribberink, 1987).

3.2.3 Oscillatory flow conditions in the test section

The longitudinal and cross-sectional variation of the oscillatory flow conditions in the test section of the tunnel was measured for one imposed sinusoidal oscillation with period $T = 8$ s and water velocity amplitude $U = 0.98$ m/s (length of the water particle excursion ≈ 2.5 m).

Figure 10 shows the longitudinal behaviour of the oscillatory flow along the complete test section as measured with the laser-doppler system along the axis of the working cross-section (i.e. 40 cm from the bottom and the roof and 15 cm from both side walls). The upper figure shows the behaviour of the horizontal velocity amplitude with distinction between the 'left' (= direction piston)

and 'right' (= direction open riser) water particle excursion. The lower figure shows the behaviour of the turbulent vertical velocity fluctuations (i.e. estimated velocity amplitude).

Although the horizontal velocity amplitude is rather uniform in the central 10 m of the test section (with no visible difference between the left and right water excursion), the uniform behaviour of the vertical velocity fluctuations is restricted to the central 7 m of the test section. A turbulence decay section appears at both ends of the test section with a length of approximately one water particle excursion length (2.5 m). Moreover, a small difference can be observed between the flow behaviour in the left and right end of the test section. This probably reflects the asymmetry of the tunnel (closed and open riser).

Figure 11 shows the cross-sectional variation of the horizontal velocity amplitude in the lower 20 cm of the measuring section in the middle of the test section ($x = 0$ m). A measuring grid was used with 5 points in the horizontal y -direction (perpendicular to the tunnel axis, $y = 5$ cm) and 5 points in the vertical z -direction ($z = 4$ cm, with the lowest point appr. 0.5 cm from the bottom). A similar grid was used at 0.4 and 1.0 m at both sides of the central position $x = 0$ m, however, the lda measurements were limited to the two central vertical and horizontal grid lines.

The measurements were carried out for the same sinusoidal oscillation as applied for the longitudinal velocity measurements ($T = 8$ s, $U = 0.98$ m/s). In each measuring point the relative deviation of the horizontal velocity amplitude from the average value (averaged over all measurements) is shown. In the lowest grid points the velocity amplitude seems to be systematically greater than the average value, which is probably related to the overshoot phenomenon in the oscillatory boundary layer. Most of the measured deviations are within the range 0 - 1%, the maximum deviation (with exclusion of the lowest grid points in the boundary layer) is 3.8%. The observed variation in the deviations has the same order of magnitude as the (random) measuring error (1 - 3%) and it is therefore concluded that the measurements give no indication for the presence of a cross-sectional or longitudinal variation of the horizontal velocity amplitude.

4. Summary and Conclusions

- A new large oscillating water tunnel was built at DELFT HYDRAULICS which enables a controlled and full-scale simulation of the wave induced oscillatory flow near the sea bed in moderate and extreme coastal conditions.
- After the realization of a number of tunnel modifications (extended vertical open riser, revision of the servo-cylinder and its suspension etc.), performance tests learned that the working range of the tunnel is in accordance with the design requirements or even exceeds them. Oscillatory flows can be realized in the tunnel in the following velocity amplitude and oscillation period range (see Fig. 5):
 - in the period range $2 < T < 5$ s maximum velocity amplitudes of 0.6 m/s ($T = 2$ s) to 1.75 m/s ($T = 5$ s) can be realized (acceleration limitation),
 - in the period range $5 < T < 8$ s maximum velocity amplitudes of 1.75 m/s can be realized (velocity limitation), and
 - in the period range $8 < T < 15$ s maximum velocity amplitudes of 1.75 m/s ($T = 8$ s) to 1.0 m/s ($T = 15$ s) can be realized (displacement limitation).
- An overview is given of the technical specifications of the tunnel as far as relevant for users of the tunnel (Chapter 2).

An electronic harmonic oscillator and a punch paper tape unit is available for the generation of controlled sinusoidal and random oscillations. The following measuring equipment is standard available:

 - a forward scatter 2DV lda system
 - a movable transverse suction system

Moreover, the piston position, the piston velocity and the driving hydraulic pressure signals are monitored.
- The amplitude and phase transfer between input signal and piston motion shows a linear behaviour (constant gain factor and phase factor) in the relevant velocity range ($U > 0.25$ m/s) and for oscillation periods $T > 6$ seconds. In the period range $T < 6$ s the gain factor shows an increase of approximately 5%. Special attention should be paid to the latter behaviour in case of the generation of random oscillations.

- The signal transfer between imposed piston velocity signal and the mean water velocity in the test section is direct, i.e. with a constant gain factor (≈ 3.27) and a negligible phase factor.
- Spectral analysis of the piston velocity signal in case of sinusoidal input signals showed the existence of some signal deformation (generation of higher harmonic oscillations).

The following contributions of the first and second higher harmonics were observed:

- < 1% for oscillation periods $T = 8, 10$ and 14 s in the velocity range $0.35 < U < 1.5$ m/s
- < 4% for all investigated periods $T = 5, 8, 10$ and 14 s, in the velocity range $0.35 < U < 1.2$ m/s
- < 8% for all investigated periods $T = 5, 8, 10$ and 14 s, in the velocity range $0.2 < U < 1.7$ m/s

The deformation is of a symmetrical type (i.e. the generated velocities during the upward and downward stroke show a similar deviation from the ideal sinusoidal shape) and is therefore of a different character than the asymmetry to be expected in field conditions (difference between onshore and offshore velocities).

- The oscillatory flow behaviour in the tunnel was studied with a number of LDA measurements in the test section for the case of an imposed sinusoidal oscillation with $T = 8$ s and $U = 1.0$ m/s. Velocity measurements along the axis of the test section showed a uniform flow behaviour along the central 7 meter of the test section. Turbulence decay sections appeared to be present on either side of the test section with a length of approximately the water particle excursion length (2.5 m). Velocity measurements in 5 cross-sections in the lower 20 cm of the central 2.0 m of the test section gave no indication for the presence of systematic variations in horizontal velocity amplitude.

REFERENCES

Bosman, J.J. (1985).

Een Grote Golftunnel ten behoeve van het onderzoek in de werkgroep Zandtransport.

Nota M1695-12, Waterloopkundig Laboratorium.

Godefroy, H.W.H.E. (1981).

Beschrijving van de tweedimensionale Laser-Doppler snelheidsmeter.

S216, WL nr. 08.02.00, Beschrijv. no. 057.

Hulsbergen, C.H. and Bosman, J.J. (1981).

Ontwerp, bouw en eigenschappen van de Golftunnel.

Verslag M1388, Waterloopkundig Laboratorium.

Jonsson, I.G. and N.A. Carlsen (1976).

Experimental and theoretical investigations in an oscillatory turbulent boundary layer.

Journ. of Hydr. Res., 14, no. 1.

King, D.B., Powell, J.D. and Seymour, R.J. (1984).

A new oscillatory flow tunnel for use in sediment transport experiments.

Coastal Engineering Conference 1984.

Ribberink, J.S. (1987).

Influence of wave-asymmetry and wave-irregularity on time and bed-averaged sediment concentrations - Wave Tunnel Experiments.

Notitie H186.00-1.

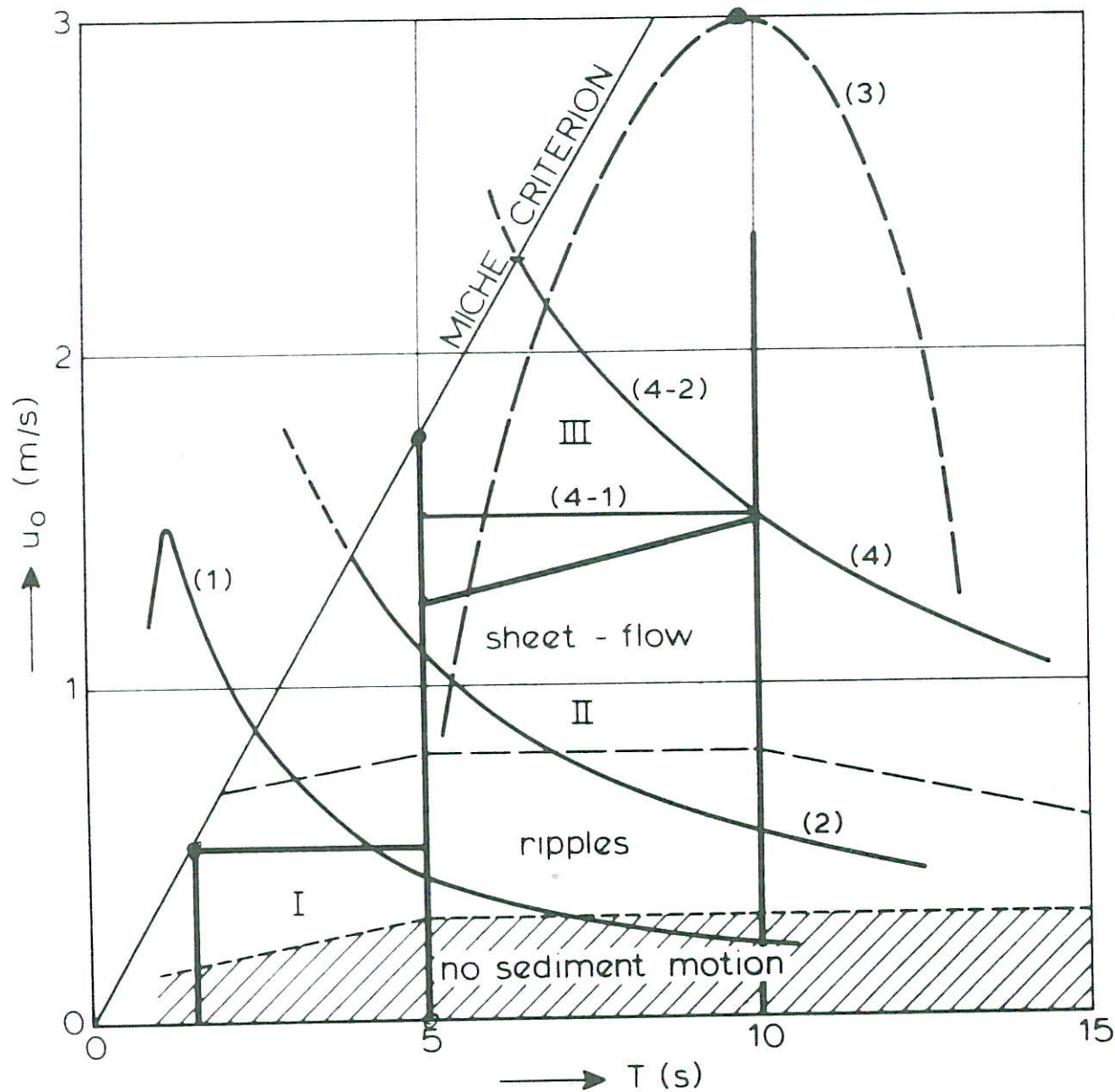


FIG. 1 DESIRED WAVE TUNNEL

- I - laboratory wave flume (except Delta flume)
- II - non-extreme coastal zone (incl. Delta flume)
- III - extreme coastal zone
- (1) - DHL - presently
- (2) - SCRIPPS
- (3) - ISVA
- (4) - DHL - desired: (4-1) : prim. requirement
(4-2) : sec. requirement

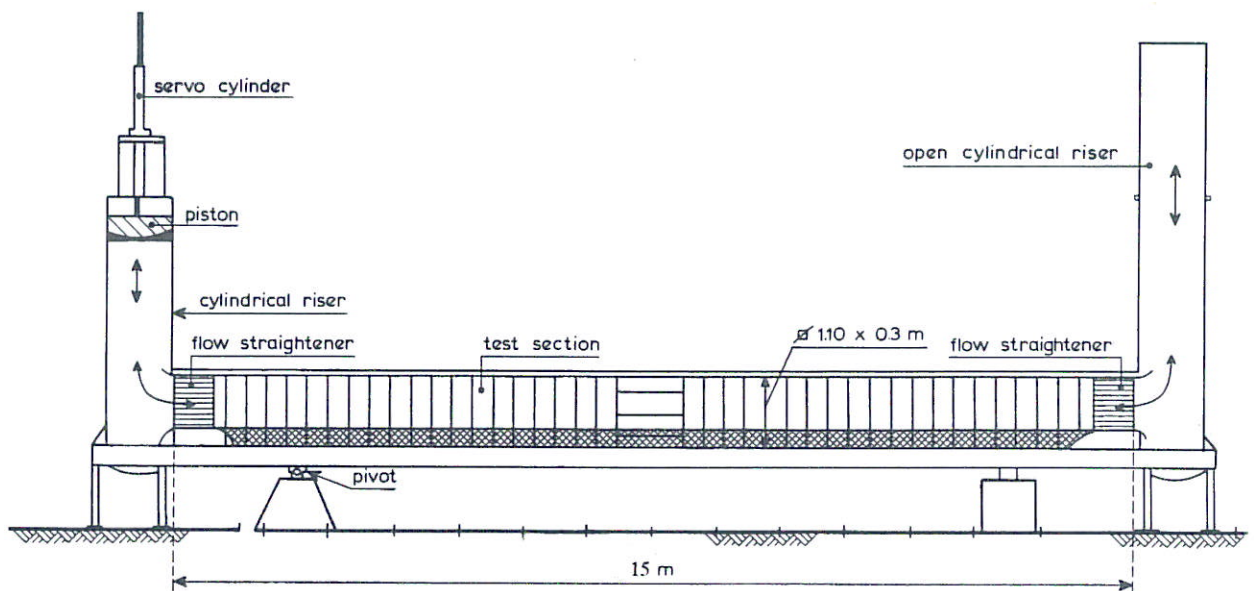
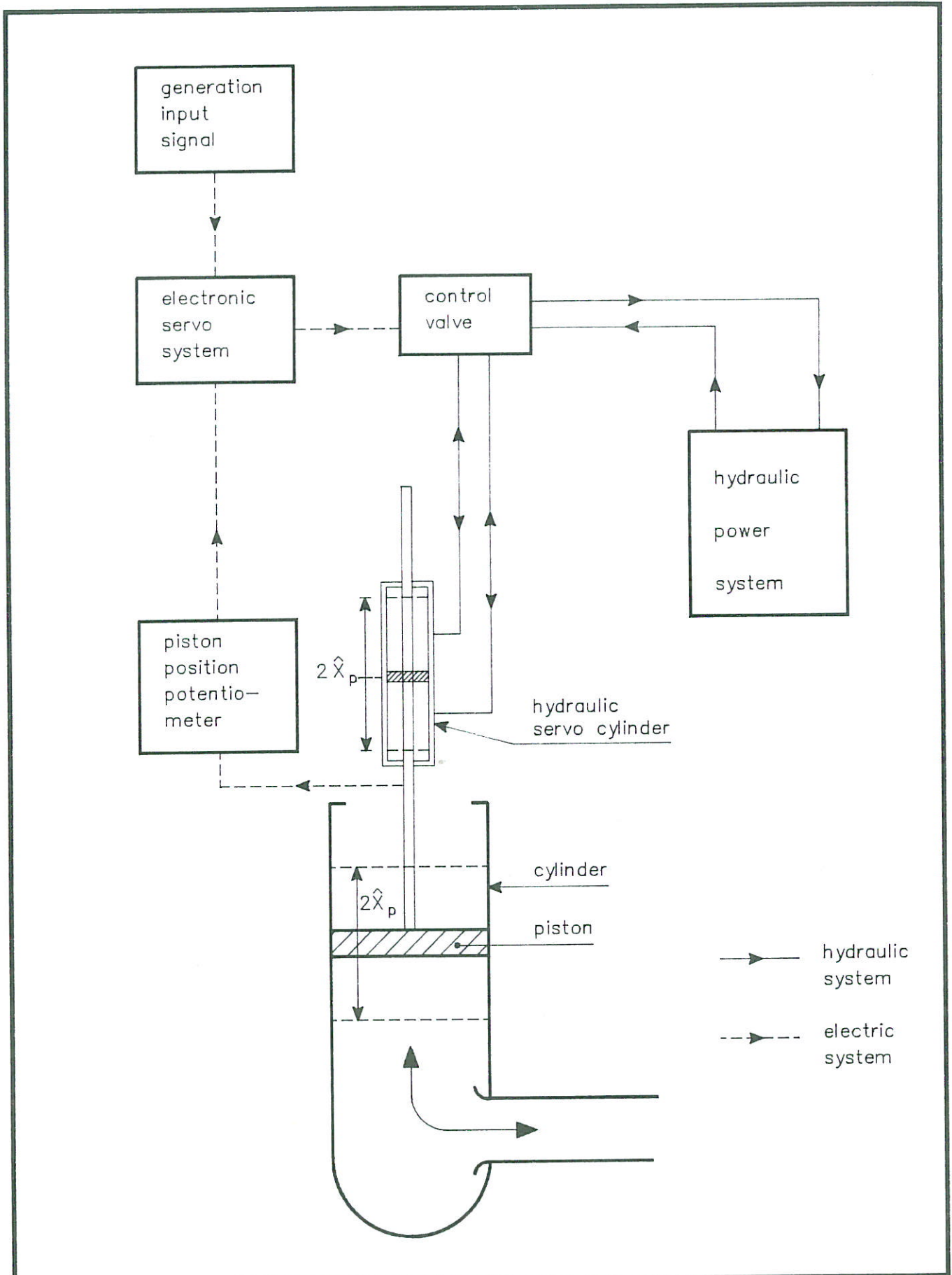
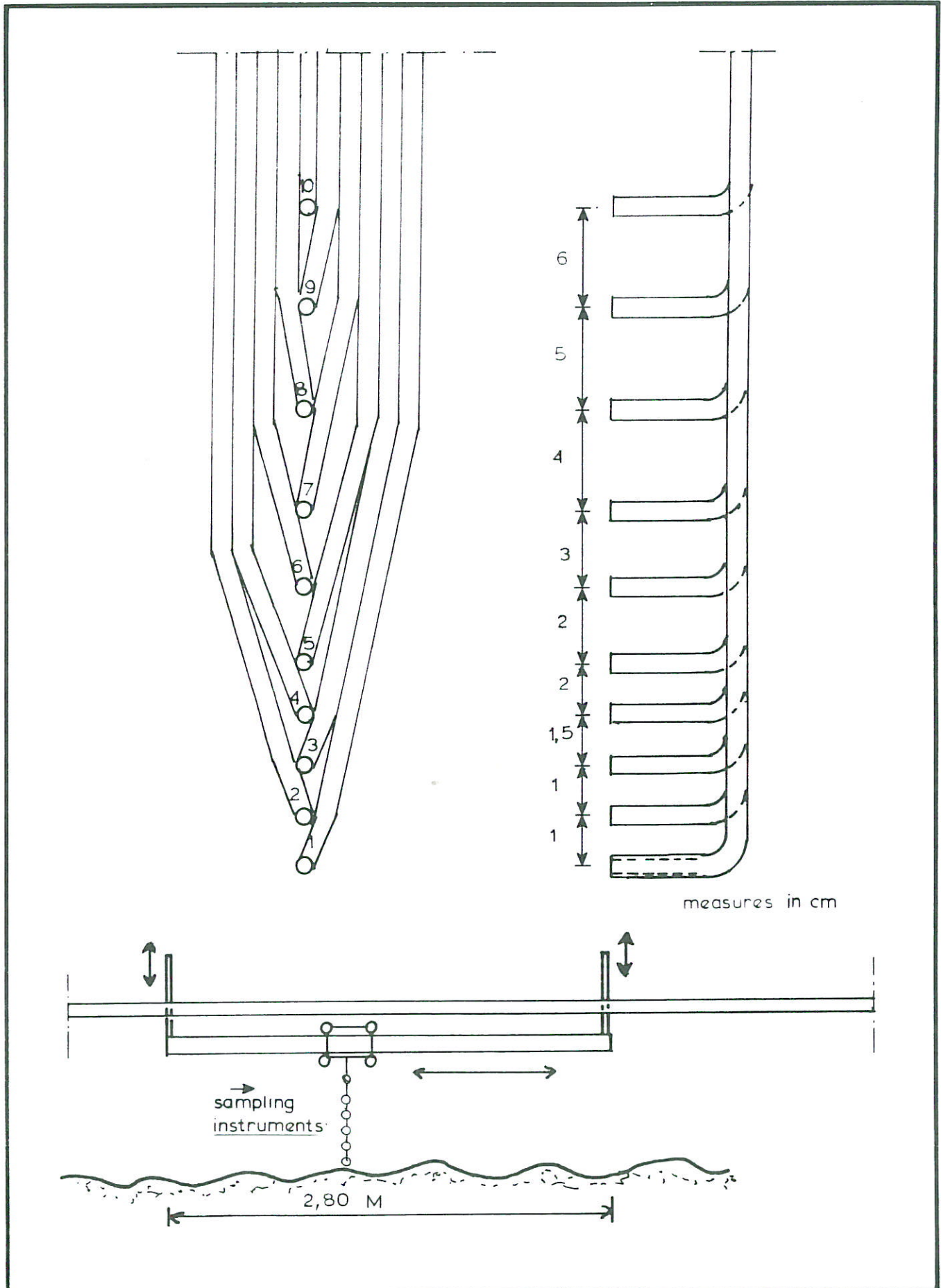


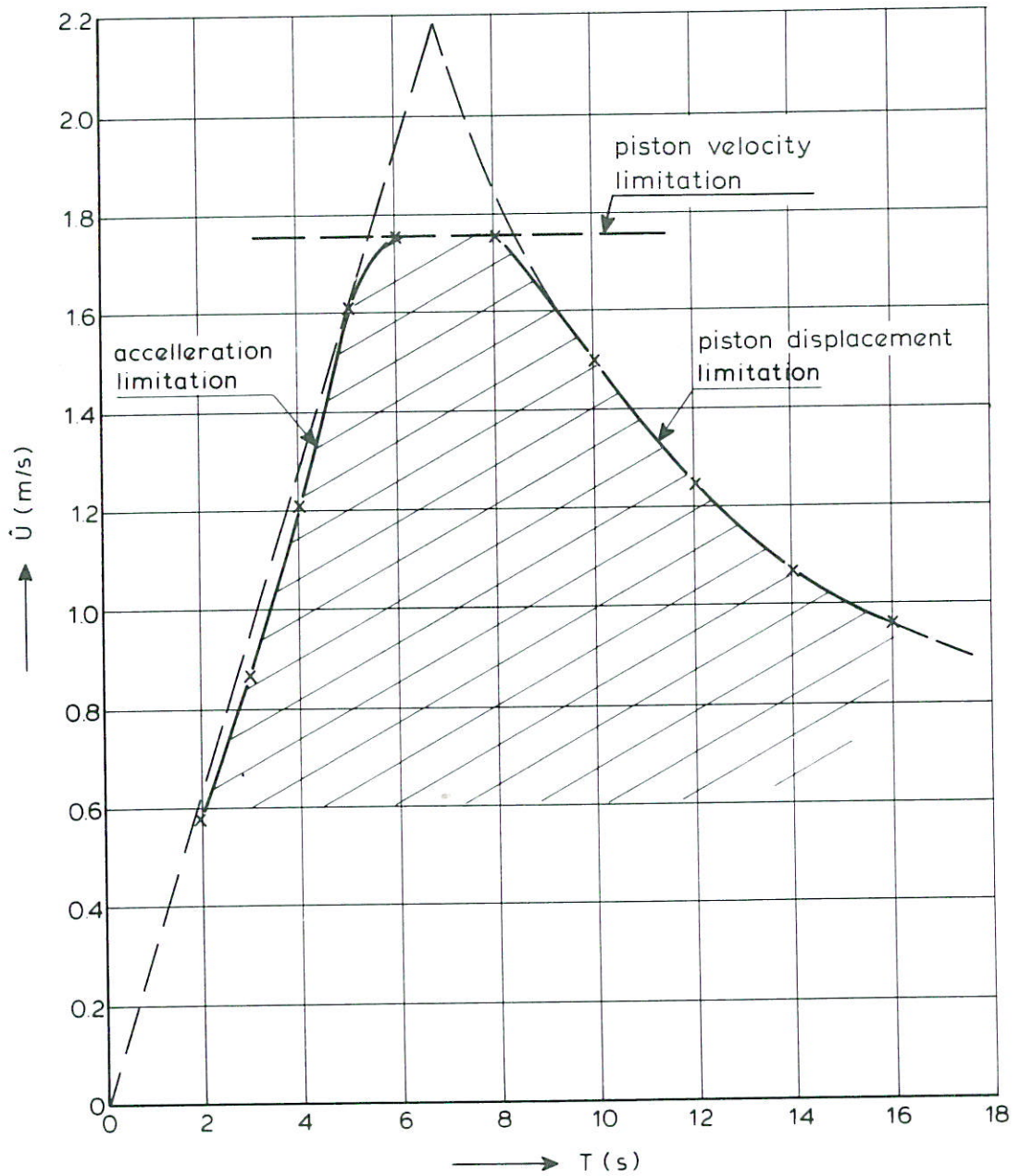
FIG. 2 OSCILLATING WATER TUNNEL (DELFT HYDRAULICS)



LARGE WAVE TUNNEL-
PISTON DRIVING SYSTEM



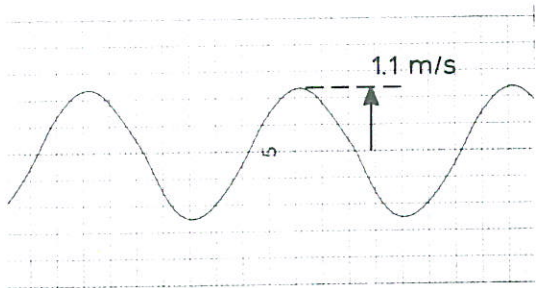
TRANSVERSE SUCTION CONCENTRATION METER



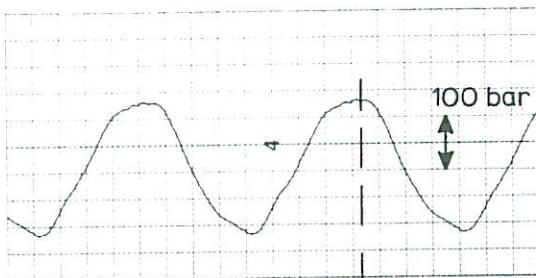
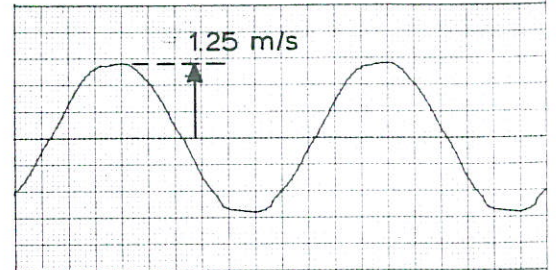
MAXIMUM VELOCITY AMPLITUDE (\hat{U}) - PERIOD (T)
 RANGE / OSCILLATING WATER TUNNEL

T = 4s

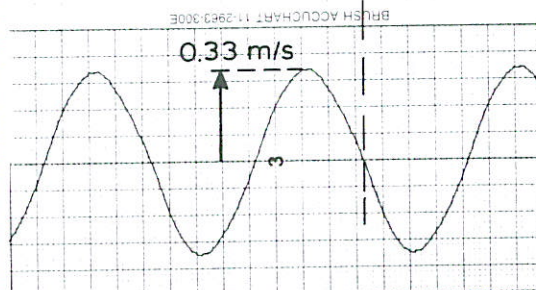
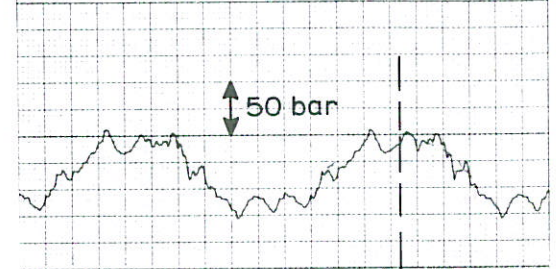
T = 10s



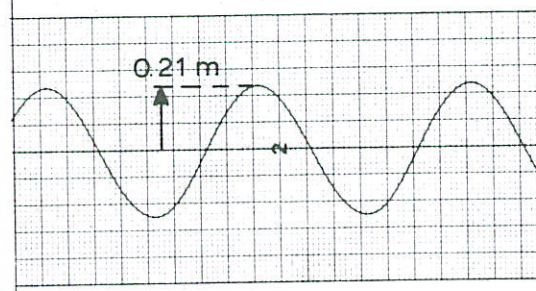
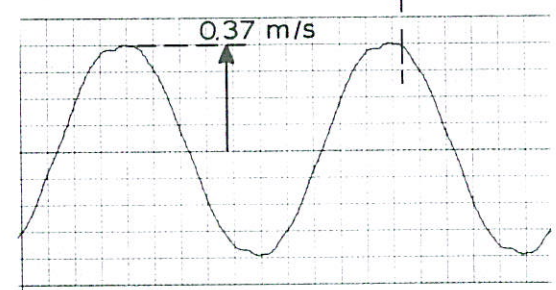
horizontal water velocity



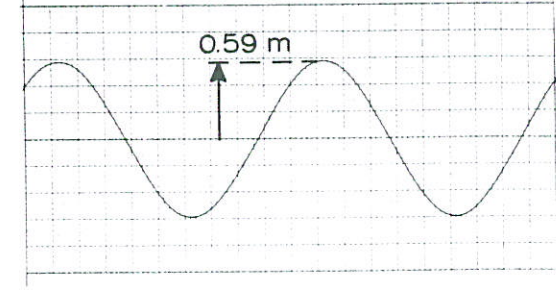
driving pressure difference



piston velocity



piston position



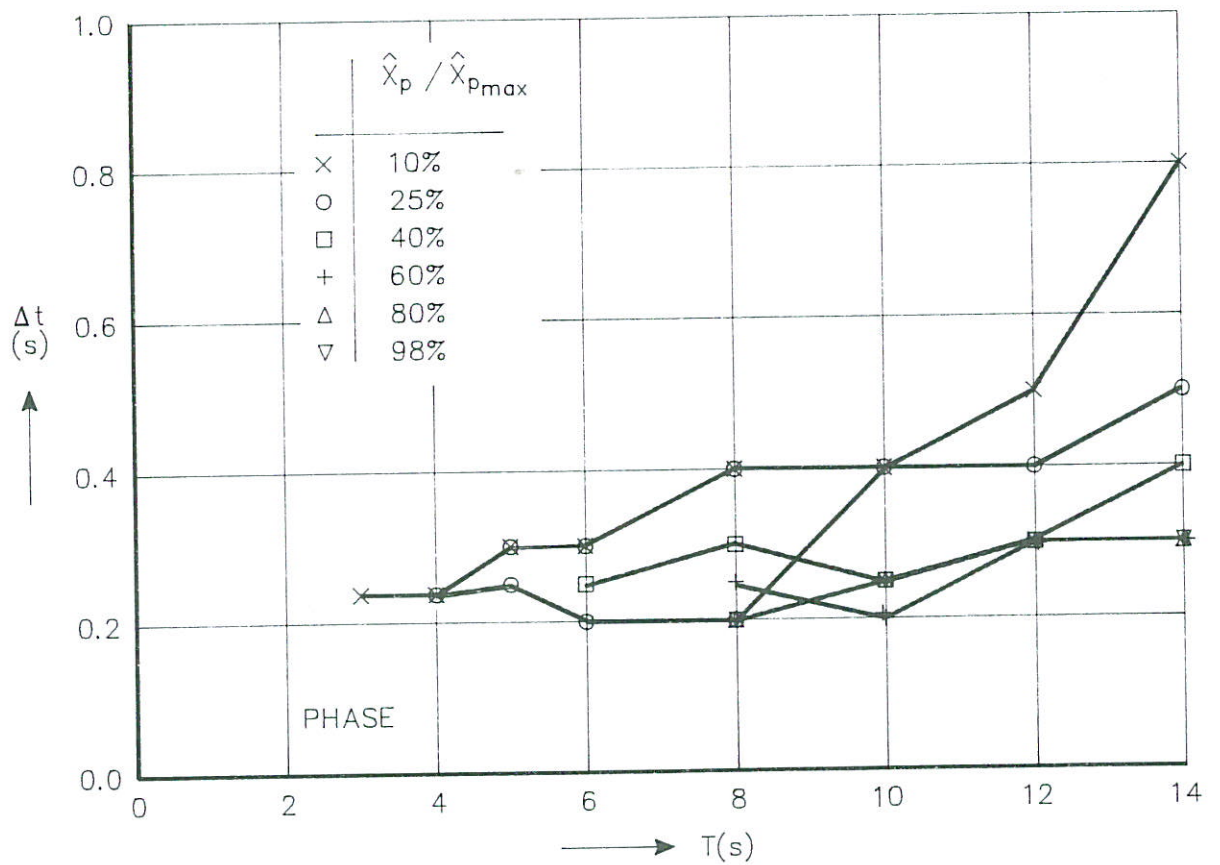
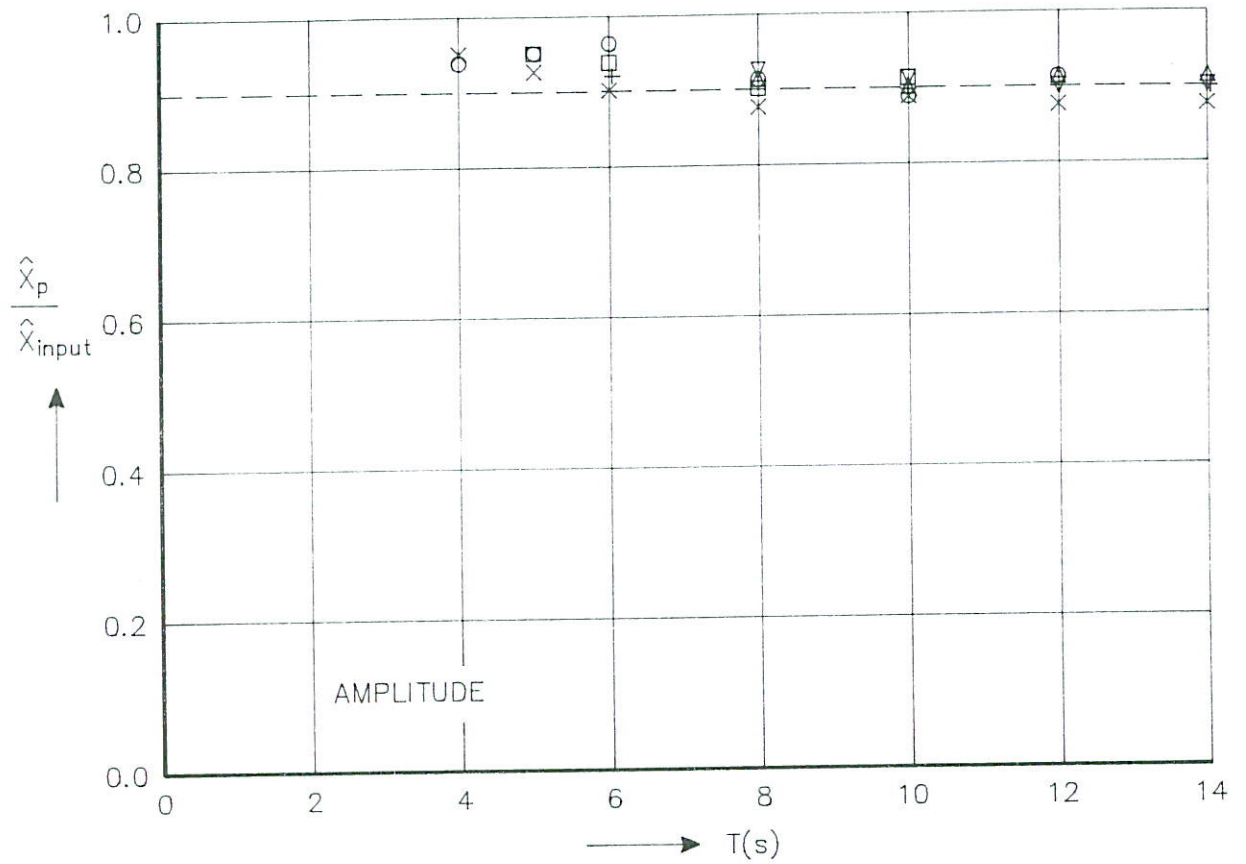
CHARACTERISTIC TUNNEL SIGNALS

2-88

DELFT HYDRAULICS

H 840

FIG. 6



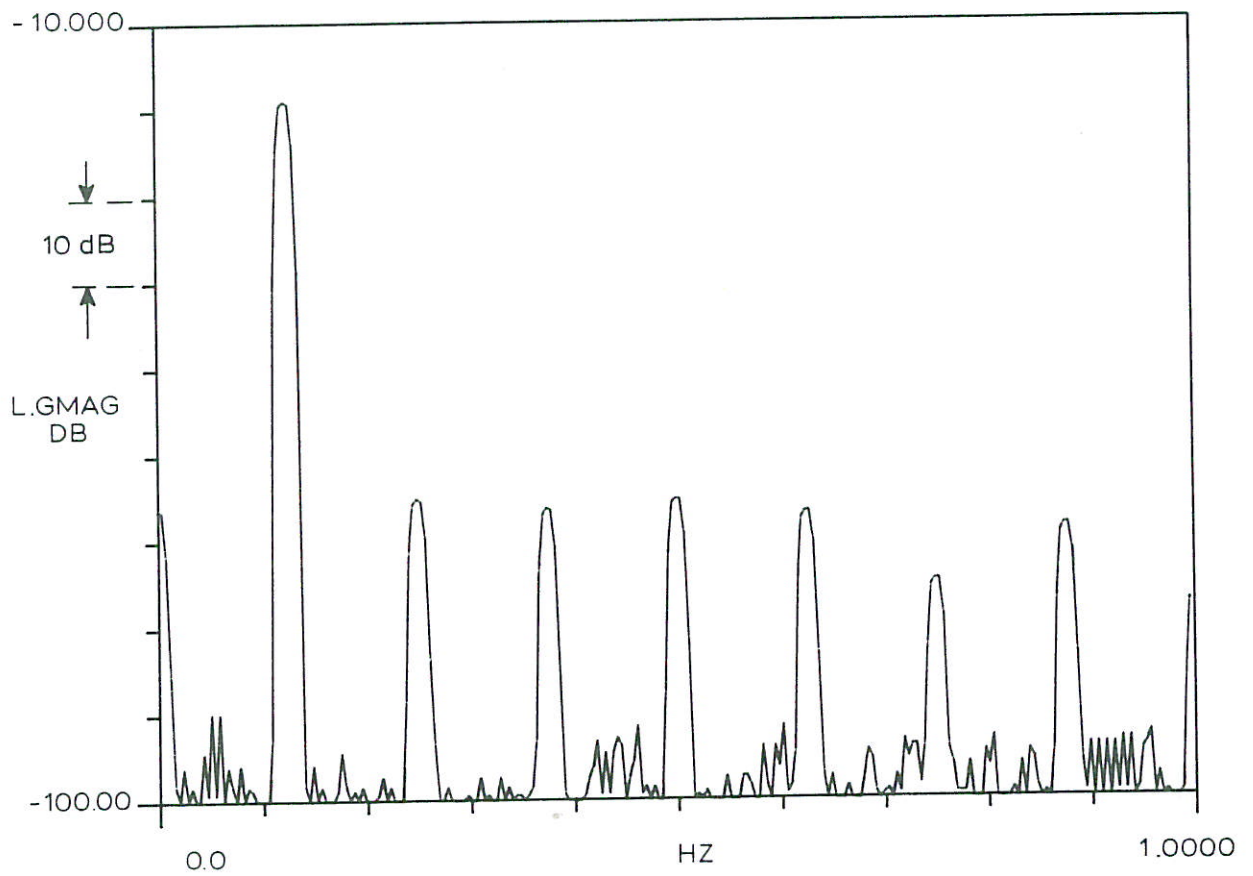
AMPLITUDE/PHASE TRANSFER
INPUT SIGNAL - PISTON DISPLACEMENT

8-87

DELFT HYDRAULICS

H 840

FIG. 7

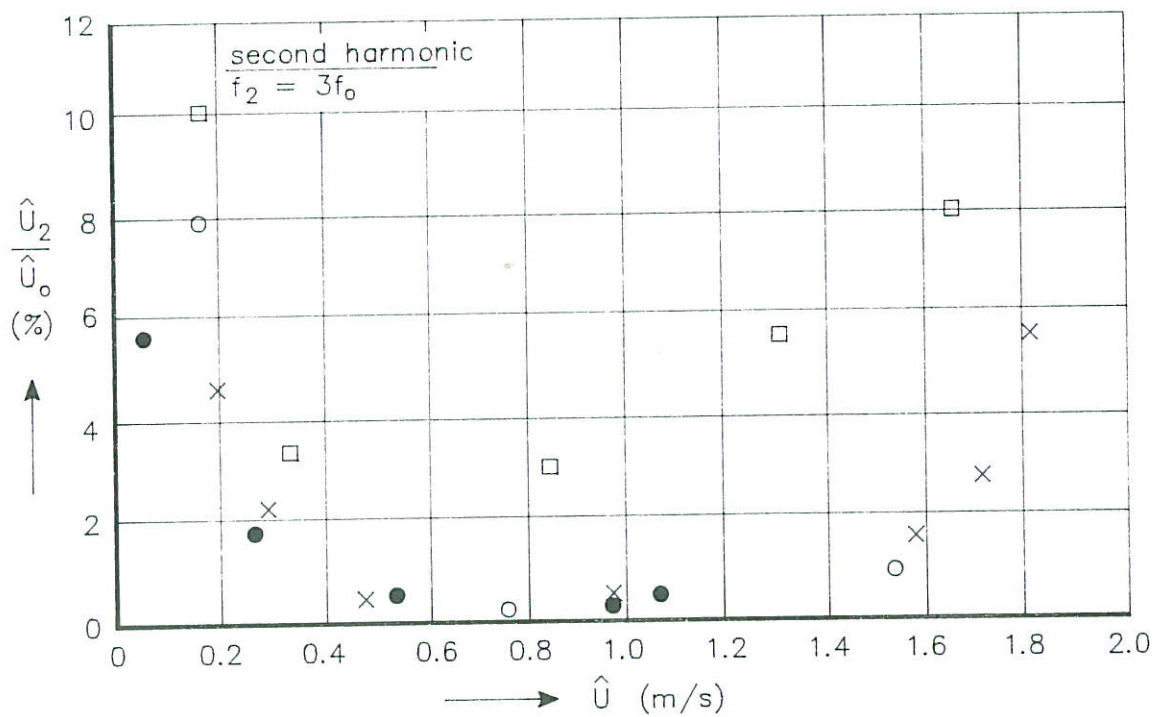
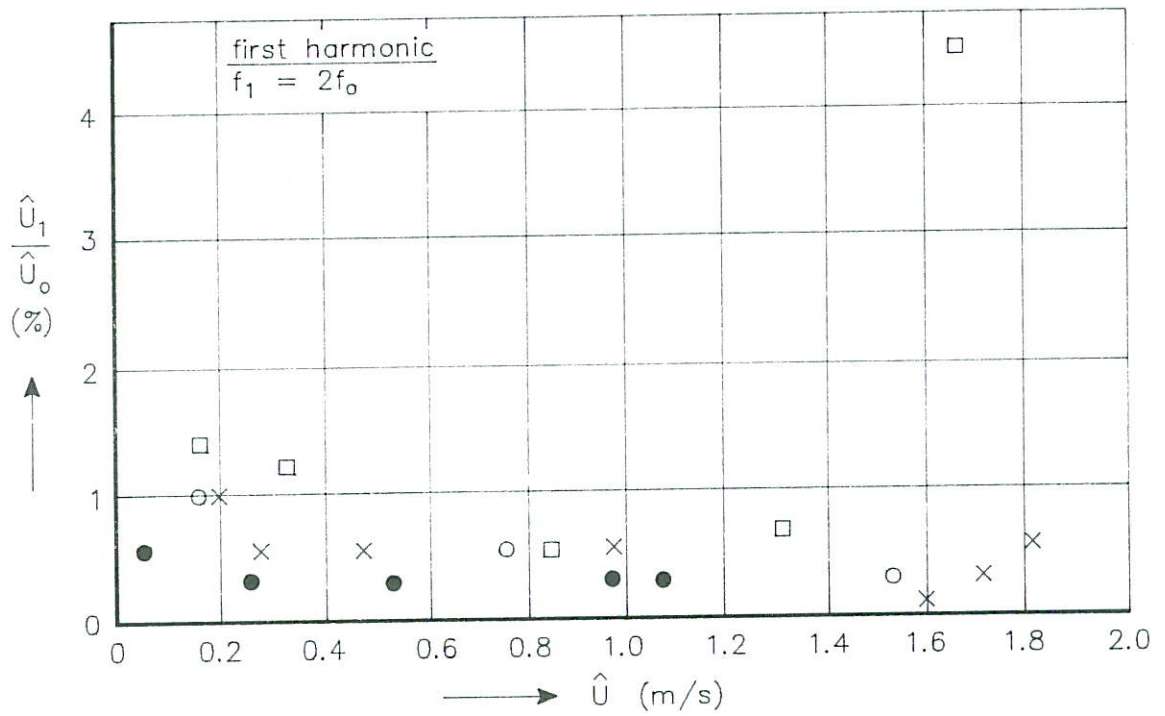


MEASURED ENERGY SPECTRAL DENSITY
 FUNCTION OF PISTON VELOCITY -
 $T = 8s$, $\hat{U} = 1.0 \text{ M/S}$

DELFT HYDRAULICS

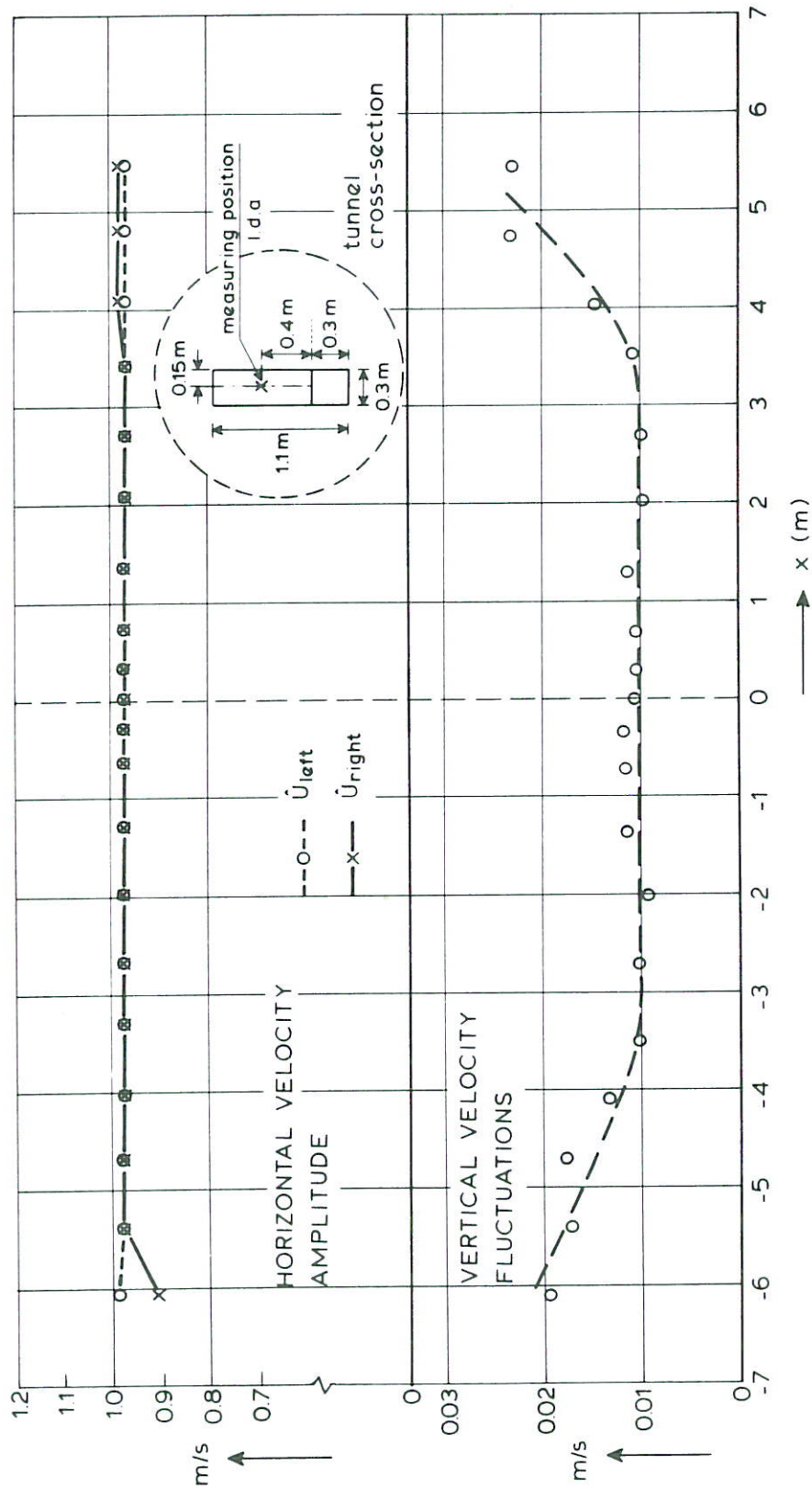
H 840

FIG. 8



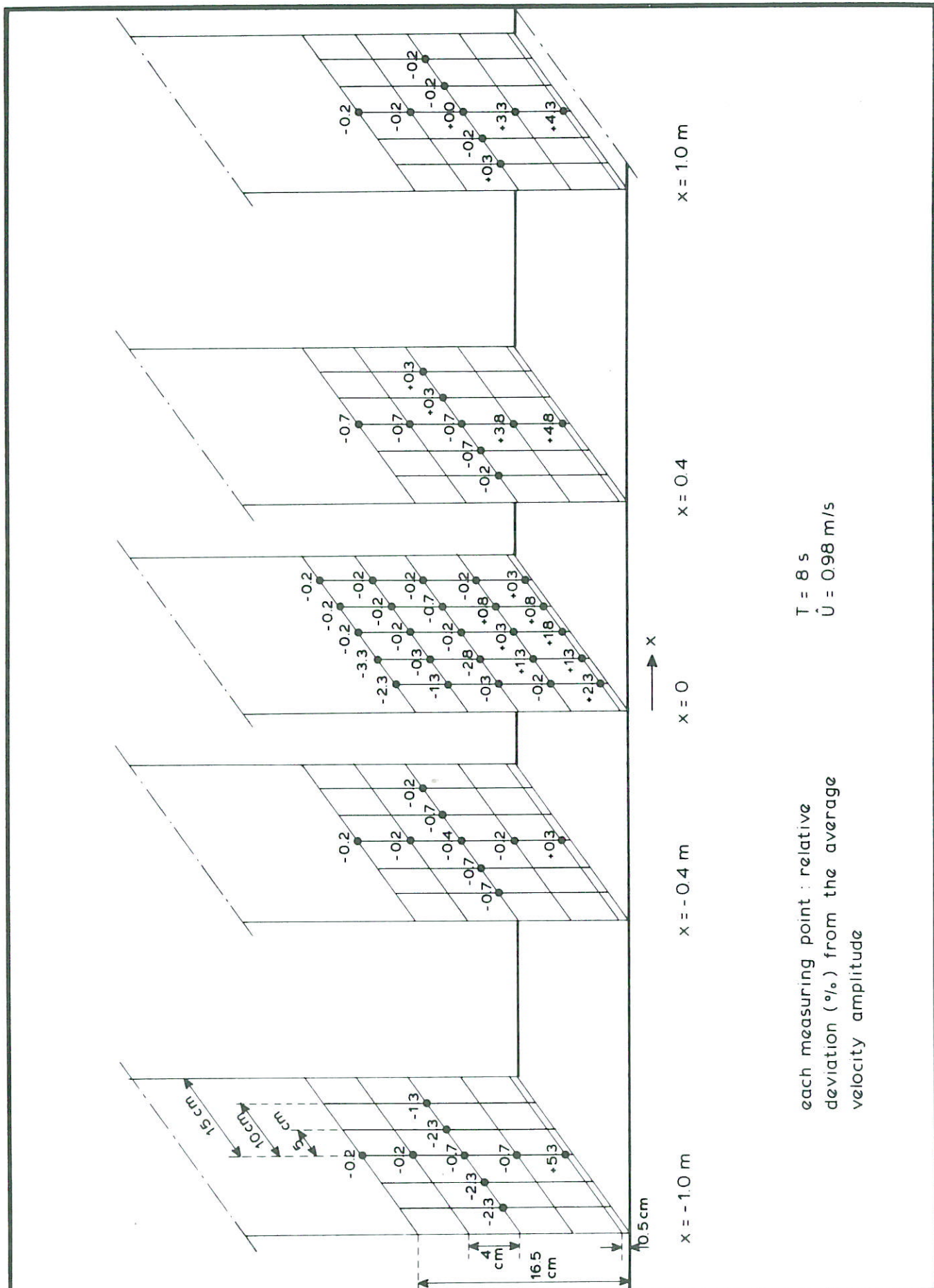
	T(s)
□	5
×	8
○	10
●	14

DEFORMATION OF PISTON VELOCITY SIGNAL



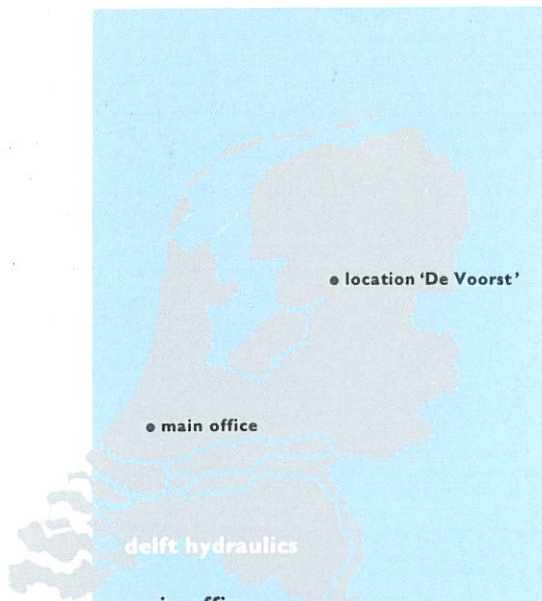
VELOCITY VARIATION ALONG WAVE TUNNEL
 AXIS, $T = 8\text{ s}$, $\hat{U} = 0.98\text{ m/s}$

10-2-88



VARIATION OF THE HORIZONTAL VELOCITY AMPLITUDE IN THE MEASURING SECTION

11-2-88



delft hydraulics
main office
Rotterdamseweg 185
p.o. box 177
2600 MH Delft
The Netherlands
telephone (31) 15 - 56 93 53
telefax (31) 15 - 61 96 74
telex 38176 hydel-nl

location 'De Voorst'
Voorsterweg 28, Marknesse
p.o. box 152
8300 AD Emmeloord
The Netherlands
telephone (31) 5274 - 29 22
telefax (31) 5274 - 35 73
telex 42290 hylvo-nl

